

# LASER INDUCED FLUORESCENCE: APPLICATION TO SPECTROSCOPY AND NEW MICROSCOPY IMAGING METHODS\*

FLUORESCENCIA INDUCIDA POR LÁSER: APLICACIÓN A LA ESPECTROSCOPÍA Y NUEVOS MÉTODOS DE IMAGINERÍA MEDIANTE MICROSCOPÍA\*

J. -P. GALAUP

Laboratoire Aimé Cotton CNRS and Paris 11 University, France jean-pierre.galaup@lac.u-psud.fr<sup>†</sup>

<sup>†</sup> corresponding author

(Recibido 13/4/2012 ; Aceptado 2/4/2013)

Laser induced fluorescence is one of the light using techniques which allows the highest sensitivity for atoms and molecules detection, up to the single atom or single molecule level. This field is much too large for an extensive review; therefore we have chosen to focus on two main points: 1- the observation of laser stimulated fluorescence in phthalocyanine and porphyrin like molecules in rare gas and nitrogen matrices at low temperatures. 2- the presentation of laser induced fluorescence techniques suitable for achieving ultra-high spatial resolution imaging, below the diffraction limit of conventional microscopy, thanks to highly fluorescent molecules to be used as biological markers.

La fluorescencia inducida por láser es una de las técnicas luminosas que permite una mayor sensibilidad en la detección de átomos y moléculas, al nivel de átomos o moléculas aislados. Este campo es muy amplio para una revisión exhaustiva, por tanto nos enfocaremos en dos puntos principalmente: 1- la observación de fluorescencia estimulada por láser en moléculas del tipo de la ftalocianina y la porfirina en matrices de gases raros y nitrógeno a bajas temperaturas. 2- la presentación de técnicas de fluorescencia inducida por láser adecuadas para alcanzar imágenes de ultra-alta resolución espacial, por debajo del límite de difracción de la microscopía convencional, gracias a las moléculas altamente fluorescentes que se usan como marcadores biológicos.

**PACS:** Fluorescence of molecules, 33.50.Dq. Stimulated emission condensed matter, 78.45.+h, Luminescence optically stimulated, 78.60.Lc.

## INTRODUCTION

Spectroscopy by Laser Induced Fluorescence (LIF) allows a wide field of applications. In chemistry and physics of plasmas, LIF serve for identifying compounds and measuring absolute concentrations of atoms and molecules in a given electronic or vibronic state. Moreover, determining local temperatures and speeds of set of particles provides information on the thermodynamic state of the system explored. Since years, LIF allowed also the high resolution study of large molecules of chemical or biological interest in supersonic jets or in solid environments cooled down to liquid helium temperatures. As an example, the fluorescence excitation and dispersed fluorescence spectra of several porphyrins was observed after the gas phase sample had been cooled in a supersonic free jet [1] or the molecules were dispersed in a solid host and cooled down to very low temperatures [2].

In this short review paper, we want to mention also other interests of this technique, mainly associated with the use of fluorescence for imaging and especially of microscopic and even nanoscale objects, below the resolution limit of a conventional microscope.

\* Artículos presentados en el VII Taller internacional TECNOLÁSER y III Reunión de Óptica, Vida y Patrimonio (La Habana, abril de 2012)

## BASIC PRINCIPLES

A scheme of LIF spectroscopy is drawn in Figure 1.

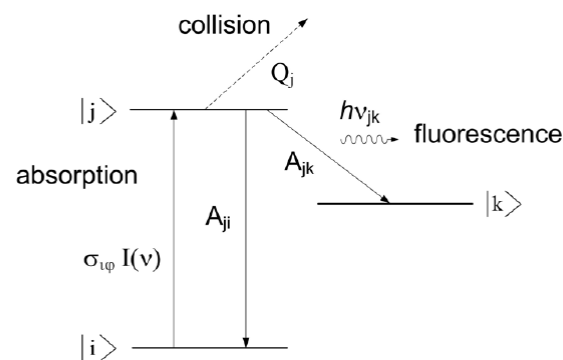


Figure 1. Schematic diagram for LIF spectroscopy.  $I(v)$  corresponds to the laser beam intensity and  $\sigma$  is the absorption cross section.  $A$  represents the probability of spontaneous transition.  $Q$  represents the "quenching", that is to say the phenomenon of non-radiative de-excitation by collisions, phonons or other molecule-molecule interactions [3].

Selective laser optical pumping realizes the population transfer from the low level  $|i\rangle$  to a higher level  $|j\rangle$ , and the flux of fluorescence photons emitted during the radiative relaxation from the level  $|j\rangle$  to an intermediate level  $|k\rangle$  is

measured. The symbolic states  $|i\rangle$ ,  $|j\rangle$  and  $|k\rangle$  of the drawing can be electronic, vibronic, vibrational, rotational states of atoms, ions or molecules. In the general case of molecules, the emissive state  $|j\rangle$  is the lowest singlet state whereas the  $|k\rangle$  state correspond to a vibrational level of the ground state  $|i\rangle$ . The radiation intensity of fluorescence emitted from the  $|j\rangle$  level provides information on the population of the initial state  $|i\rangle$ . We remind also that the measured lifetime of the fluorescence from the  $|j\rangle$  level includes also the non-radiative contribution due to collision processes in gas phase or phonon perturbations or molecule-molecule interactions in solid states: one talk about the phenomenon of quenching.

Rather simple considerations allow evaluating the flux of fluorescence photons  $n_{flu}$ . Naming  $N_i$  (respectively  $N_j$ ) the density of molecules in the  $|i\rangle$  (respectively  $|j\rangle$ ) state, in the case where  $N_i \gg N_j$ , the total number of fluorescence photons  $n_{flu}$  is proportional to the integral over spectral and time domains of the convolution product between the spectral profile  $P_{abs}$  of the optical transition  $|j\rangle \leftarrow |i\rangle$  (absorption spectrum) and the spectral profile  $P_L$  of the laser, such that:

$$n_{flu} = KN_i \frac{A_{jk}}{A_j + Q_j} \sigma_{ij} \iint \frac{P_{abs} \otimes P_L}{h\nu} I_L(t) d\nu dt \quad (1)$$

In this expression,  $K$  is constant of proportionality,  $A$  is the Einstein's coefficient for spontaneous emission,  $Q$  is the term for quenching,  $\sigma_{ij}$  is the absorption cross section and  $I_L$  is the laser intensity. As shown by this equation, the fluorescence signal depends on the lifetime  $\tau_j$  of the emissive level  $|j\rangle$  ( $\tau_j = 1/(A_j + Q_j)$ ), the absorption cross section, the density of the initial state, the laser intensity and the absorption and the laser spectral profiles. Under the conditions of the linear absorption regime, the fluorescence signal varies linearly with the intensity of the laser beam. Notice that all the information concerning the  $|j\rangle$  level is actually contained in the absorption profile  $P_{abs}$ .

In practice, a typical set-up for a LIF experiment is shown in Figure 2.

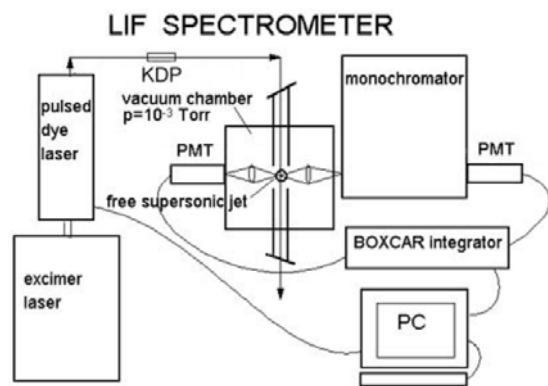


Figure 2. Typical schematic diagram for LIF experiment applied to jet cooled systems. Important is the tunable laser source constituted by a nanosecond excimer laser for pumping the dye laser eventually followed with a KDP non-linear crystal for frequency doubling [4].

The important points for such an experiment is the tunable laser source, the experimental chamber where is located the

system under study and a monochromator with a detector device. The most common laser is a nanosecond pulsed dye laser system which allows large tunability over the visible range depending on the dye used. At present, also tunable all solid laser sources using only non-linear crystals and OPO/OPA designs are under constant development. The experimental chamber can be a simple gas cell, a supersonic jet under vacuum or a cryostat for cryogenic systems. The detectors are photomultipliers, avalanche photodiodes or CCD cameras

## LASER STIMULATED FLUORESCENCE

Recent luminescence works [5,6] on porphyrin and phthalocyanine-doped cryogenic matrices have revealed the occurrence of stimulated emission for specific vibronic transitions under selective laser excitation. This phenomenon was characterized by a drastic intensity increase of a specific vibronic fluorescence line with only a moderate increase of the laser pump intensity. The most concerned transition was assigned as the one taking place between the first excited electronic state and a vibrational level of the ground state located at approximately 1550 and 1525  $\text{cm}^{-1}$  in  $\text{H}_2\text{Pc}$  and  $\text{ZnPc}$  respectively [5].

Further experiments revealed that the stimulated emission observed for phthalocyanines in cryogenic matrices is a more general behavior that was also observed in the case of porphyrin molecules belonging to the tetrabenzoporphyrin family [6]. Indeed, tetrabenzoporphyrin (TBP) molecules have the closest structure to the phthalocyanines (Pc), the most noticeable change being the replacement of the four bridging nitrogen atoms belonging to the internal ring by carbon atoms. Therefore, similar vibronic structures are expected between both species.

We summarize here the most important results obtained. Laser Induced Fluorescence spectroscopy is very well adapted for studying these molecules because most of their absorption bands in the visible region closely match the working range of tunable dye lasers. While undertaking such LIF on matrix-isolated free-base phthalocyanine ( $\text{H}_2\text{Pc}$ ) and zinc phthalocyanine ( $\text{ZnPc}$ ), by means of emission-excitation spectra using pulsed dye lasers for excitation, an unusually intense vibronic band was observed with slightly increased laser power. This novel solid state effect, which had never been reported before, was the subject of our previous paper [5]. The band involved corresponded to the transition from the first excited electronic state to a vibrational level of the ground state at approximately 1550  $\text{cm}^{-1}$ . The drastic intensity enhancement was attributed to the occurrence of stimulated emission (SE) on the basis of the following observations: 1- the laser power dependence of the phenomenon exhibits a well-defined threshold, 2- there is also a threshold as a function of the concentration of dopants, 3- the emission band is narrow compared to the spectral width of the standard fluorescence, even in the case of broad bands in the absorption spectrum, 4- its lifetime is shortened greatly in comparison with other

vibronic transitions of the emission spectrum and exhibits a perfect synchronism with the exciting laser pulses [5].

Experimental details are fully described in previous published papers and most significant recent results obtained for H<sub>2</sub>TBP and ZnTBP isolated in Ar and N<sub>2</sub> hosts are briefly presented and discussed below.

First, we can ascertain that the absorption spectrum of H<sub>2</sub>TBP/Ar corresponds to well-isolated guest molecules. The two main bands appearing at about 654 nm (15284 cm<sup>-1</sup>) and 584 nm (17132 cm<sup>-1</sup>) belong to absorptions of the split Q band, frequently labeled as the Q<sub>x</sub> and Q<sub>y</sub> bands respectively, in order of increasing energy. The two corresponding bands in the H<sub>2</sub>Pc/Ar absorption spectrum are located at about 677 nm (14771 cm<sup>-1</sup>) and 635 nm (15748 cm<sup>-1</sup>). The shift of the absorption bands observed between H<sub>2</sub>TBP and H<sub>2</sub>Pc results from the change in energy of the molecular orbitals due to the replacement of the interpyrrolic carbons by the nitrogen atoms. As a consequence, the H<sub>2</sub>Pc Q-bands are shifted to the red while the B-bands in the Soret's region are oppositely blue shifted.

In the singlet fluorescence spectra shown for H<sub>2</sub>TBP and ZnTBP in Ar host at 5 K, the higher energy band at 654.2 nm corresponds to the 0-0 zero-phonon origin band. Its structure suggests the presence of several marked sites as also noticed from the absorption spectrum. Besides the rather intense electronic origin region, the most intense band which appears in the H<sub>2</sub>TBP/Ar spectrum is that centered at 731.9 nm (13663 cm<sup>-1</sup>), revealing, like in the case of H<sub>2</sub>Pc, the existence of stimulated emission in a 4-level scheme involving a vibronic transition from the lowest electronic state to a vibrational level of the ground state.

As was noted in [7,8], the 1620 cm<sup>-1</sup> vibration of H<sub>2</sub>TBP corresponds to the A<sub>g</sub> stretching vibration of the CaCm bonds, *i.e.* to the vibration which is localized in the CaCmCa bridges in H<sub>2</sub>TBP (Ca-carbon atom in the α-position of the pyrrole rings, C<sub>m</sub>-carbon atom in the meso-position (CaCmCa bridges).

Upon increasing up the pump power intensity by a factor of about ten, from tens of μJ/pulse to hundreds of μJ/pulse, the emission band at about 732 nm gained enormously in intensity while the others remained unchanged or diminished slightly. Moreover, the linewidth of this emission band was reduced considerably while its intensity increased. The width of the band is approaching that of the exciting laser, decreasing from approximately 8 cm<sup>-1</sup> to 2 cm<sup>-1</sup>, a value surely limited by the resolving power of the monochromator.

The results summarized here confirm that the phenomenon of stimulated emission firstly observed for phthalocyanines in cryogenic matrices under modest conditions of pulsed laser excitation is not an exception. With free-base H<sub>2</sub>TBP, stimulated emission was observed in Ar and N<sub>2</sub> matrices, but not in Xe matrices. The vibronic transition involved is, , the

one involving a mode at about 1620 cm<sup>-1</sup>, a particularly active mode corresponding to the stretching Ag-vibration of the CaCm bonds, like in the case of H<sub>2</sub>Pc where the corresponding vibrational mode is at about 1550 cm<sup>-1</sup>. From all results we have obtained on stimulated emission in cryogenic matrices, with H<sub>2</sub>Pc, ZnPc as well as H<sub>2</sub>TBP, we can reasonably predict that stimulated emission should also be observable for these molecules isolated in other solid materials that also produce narrow linewidths such as Shpol'skii matrices, like n-octane. Other possible interesting candidates could also be sol-gel or polymer hosts.

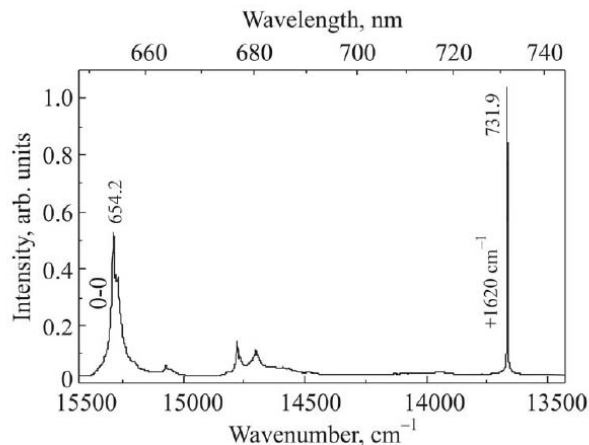


Figure 3. Typical schematic diagram for LIF experiment applied to jet cooled systems. Important is the tunable laser source constituted by a nanosecond excimer laser for pumping the dye laser eventually followed with a KDP non-linear crystal for frequency doubling [4].

## LASER FLUORESCENCE IMAGING: BEYOND THE DIFFRACTION LIMIT

Nowadays, due to the discovery of an increasing number of highly fluorescent molecules for covering large field of applications, fluorescence is becoming a powerful tool also for imaging and especially, microscopy imaging particularly for biological studies. Owing to the recently discovered Green Fluorescent Protein which is fully biological compatible, the field is in constant expansion [9]. Interestingly, is the emergence of new super-high resolution methods to overcome the spatial resolution limit of conventional microscope due to light diffraction. Among all the ideas which are under development, we want to mention here only two of them which are known under their acronyms and briefly described below: STED and STORM.

(a) **STED: STimulated Emission Depletion** The original idea of STED, introduced in 1994 [10] is that the fluorescence focal spot can be extremely sharpened by selectively inhibiting the fluorescence on its outer part with a second laser beam at the appropriate wavelength [11]. As shown in the Figure 4, one laser has a Gaussian beam as in most of the conventional laser source, whereas the second laser, at a different wavelength has a donut shaped laser beam (Laguerre-Gauss laser mode).

The influence of the stimulated emission induced by the donut beam is roughly explained as follows: 1) After excitation

by the first laser, the molecule releases its energy normally in a photon of fluorescence. 2) However, it can be “forced” back to the ground state by stimulated emission. In a STED microscope, the excitation laser is pulsed. During the brief normal fluorescence lifetime (~1 ns), a STED pulse is sent. The donut shape of the STED beam around the excitation focal point and the nonlinearity of the STED effect increase the spatial resolution by reducing the effective PSF (Point Spread Function) of the fluorescent spot. While the STED beam itself is still diffraction-limited, increasing the intensity saturates the depletion efficiency distribution: even areas close to the minima of the STED beam profile are now sufficiently bright to virtually switch off all fluorescence. This restricts the remaining fluorescence to smaller and smaller volumes - ultimately only the spots of zero STED intensity remain fluorescent. The advantage of STED on the axial resolution is expressed by comparing the following equations:

$$\begin{aligned} \text{Confocal } \Delta d &= \frac{\lambda}{2n \sin \alpha} \\ \text{STED } \Delta d &= \frac{\lambda}{2n \sin \alpha \sqrt{1 + I/I_{sat}}} \end{aligned} \quad (2)$$

where  $I_{sat}$  means the laser STED intensity at saturation. In practice, spatial resolutions down to 20-30 nm, achieved with visible wavelengths, have been demonstrated by STED in a laser scanning microscope [13].

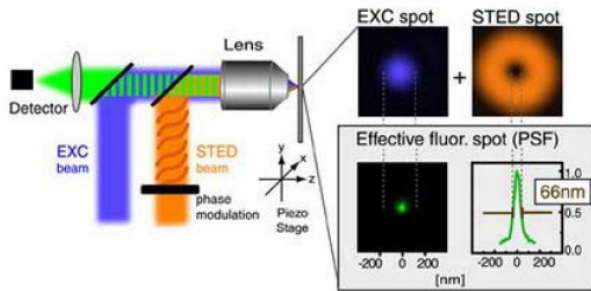


Figure 4: Scheme of a STED microscope. Two lasers are needed, one as usual with a Gaussian beam, a second one, the STED laser, with a donut shaped beam. Both lasers are pulsed [12].

(b) *STORM: STOchastic Optical Reconstruction Microscopy* In conventional fluorescence microscopy, a large number of fluorescent molecules are visible at a given time. Whenever two molecules are within the diffraction limited spot of one another, they cannot be distinguished as separate individuals. As a result, normal fluorescence images are blurred by diffraction and features smaller than the point spread function are lost.

In contrast, single fluorescent molecules can be localized with a much better precision, smaller than the diffraction limited resolution. Therefore, the principle of STORM microscopy is as follows: molecules of interest in the system to be imaged with very high spatial resolution are labeled with photo-switchable fluorophores which are initially in the non fluorescent state (Fig. 5-a). Using a pulsed laser source at a convenient wavelength, in a first activation cycle, a set of fluorophores is activated to the fluorescent state but such that

the diffraction-broadened spot of each fluorophore does not overlap. From the consideration that each spot originate from a unique activated fluorophore, the fluorescent probe is then assumed to be in the centre of the spot, marked with a black cross ((Fig. 5-b). In a subsequent activation cycle, a different set of fluorophores is activated and their positions are determined as before (Fig. 5-c). Finally, after a sufficient number of cycles, an image is constructed by plotting the red dots corresponding to the measured positions of the fluorophores (Fig. 5-d). The resolution of this image is then not limited by diffraction, but by the precision of each fluorophore localization and by the number of fluorophore positions obtained.

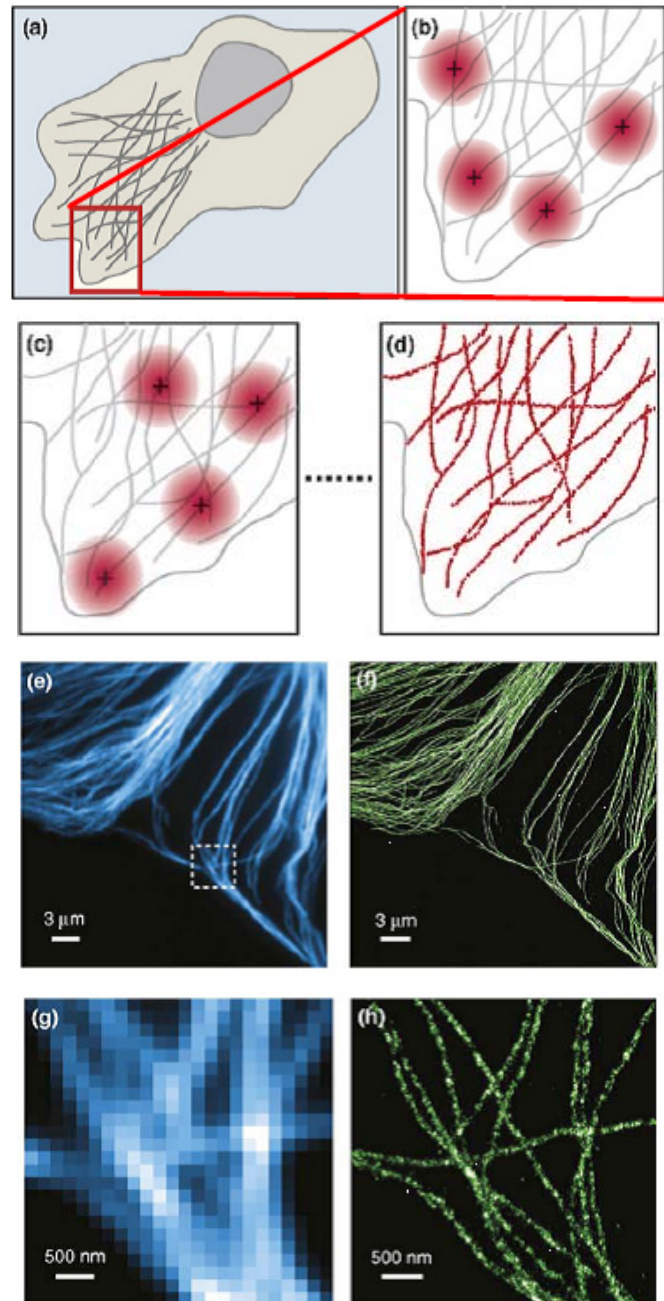


Figure 6: a-d) Principle of STORM and the reconstruction of a super-high spatially resolved image. e-h) Comparison of conventional immunofluorescence images of microtubules in a BS-C-1 mammalian cell (e and g) and STORM images (f and h) of the same areas.

An example of a result achieved using STORM is shown in

Figure 6. In the STORM images (Fig. 6-f and Fig 6-h), each localization is rendered as a Gaussian peak whose width corresponds to the theoretical localization precision. The areas shown in Fig 6-g and Fig 6-h are expanded views of the region defined by the dashed box in Fig. 6-e. The microtubules are immunolabeled with photo-switchable cyanine Cy3-Alexa 647 dye pairs. [14].

These powerful methods require the use of photoactive fluorescent probes. The choice of an appropriate probe depends on the knowledge of its photophysical properties and on the desired application. Probes with high photoactivation yields are desirable for controlling the number of active molecules. Particularly powerful probes are the genetically-encoded photoactive and photo-switchable proteins (PA-FPs) derived from the Green Fluorescent Protein (GFP) and other fluorescent proteins. Several criteria are advantageous for any photoactive probe: strong absorption coefficient at the activation and readout wavelengths, large fluorescence quantum yield in the active state, no or only a little tendency for self-aggregation, a small but finite quantum yield for photobleaching, also, for biological applications the probe emission should be separable from known intrinsic fluorescence and other sources of background. Notice that photoactivatable quantum dots would potentially be quite powerful, because of their resistance to photobleaching, as long as they could be targeted to the desired structure.

## CONCLUSIONS

Through this short review, we wanted to emphasize on the increasing importance of Laser Induced Fluorescence, as well as in the field of high resolution spectroscopy or also, due the fluorescence revolution allowed after the discovery of new and fully biologically compatible new families of extremely active fluorescent probes, in new super-high resolved microscopy imaging methods.

## ACKNOWLEDGEMENTS

C. Crépin, N. Shafizadeh, W. Chin from Institut des Sciences Moléculaires d'Orsay, Bât. 210, CNRS and Université Paris-Sud 11, 91405 Orsay cedex, France, J.G. McCaffrey from

Department of Chemistry, National University of Ireland, Maynooth, Ireland and S.M. Arabei from Belarusian State Agrarian and Technical University, Minsk, Belarus are gratefully acknowledged.

- [1] U. Even, J. Magen, J. Jortner, J. Friedman, H. Levanon, *J. Chem. Phys.* **77**, 4374 (1982); U. Even, J. Magen, J. Jortner, J. Friedman, *J. Chem. Phys.* **77**, 4384 (1982); U. Even, J. Jortner, *J. Chem. Phys.* **77**, 4391 (1982).
- [2] A. Singh, W.Y. Huang, R. Egbujor, L.W. Johnson, *J. Phys. Chem. A* **105**, 5778 (2001).
- [3] S. Mazouffre, "Spectroscopie de fluorescence induite par diodes laser: Application au diagnostic des plasmas", in *Plasmas Froids : Systèmes d'analyse, Modélisation et Rayonnement*, Publications MRCT du CNRS (2009) p. 67 (in french)
- [4] From : <http://www.fi.tartu.ee/labs/ltl/images/lif.jpg>
- [5] N. Dozova, C. Murray, J.G. McCaffrey, N. Shafizadeh, C. Crépin, *Phys. Chem. Chem. Phys.* **10**, 2167 (2008).
- [6] C. Crépin, N. Shafizadeh, W. Chin, J.-P. Galaup, J.G. McCaffrey, S.M. Arabei, *Low Temperature Physics* **36**, 451 (2010).
- [7] S.M. Arabei, K.N. Solovyov, Yu.I. Tatulchenkov, *Optics and Spectroscopy* **73**, 406 (1992).
- [8] S. F. Shkirman, L. L. Gladkov, V. K. Kostantinova and K. N. Solovyev, *Spectrosc. Lett.* **31**, 1749 (1998).
- [9] Fabienne Merola, Bernard Levy, Isabelle Demachy, and Helene Pasquier, "Photophysics and spectroscopy of fluorophores in the Green Fluorescent Protein family", in *Advanced Fluorescence Reporters in Chemistry and Biology I: Fundamentals and Molecular Design*, A.P. Demchenko (ed.), Springer Series on Fluorescence, Vol. 8 (2010) p. 347-384.
- [10] S.W. Hell, J. Wichmann, *Opt. Lett.* **19**, 780 (1994).
- [11] K.I. Willig, J. Keller, M. Bossi, S.W. Hell, *New J. Phys.* **8**, 106 (2006).
- [12] G.J. Simpson, *Nature* **440**, 879 (2006).
- [13] V. Westphal, S.W. Hell, *Phys. Rev. Lett.* **94**, 143903 (2005).
- [14] M. Bates, B. Huang, G.T. Dempsey, X. Zhuang, *Science* **317**, 1749 (2007).